

Part Decomposition and Description of 3D Shapes*

Hillel Rom[†] and Gérard Medioni
Institute for Robotics and Intelligent Systems
University of Southern California
Los Angeles, California 90089-0273
Email: rom@iris.usc.edu

Abstract

We address the problem of obtaining natural (intuitive) descriptions of 3D shapes. We present one of the first attempts to address the description of 3D compound objects, where the parts are connected smoothly. The input we consider is either complete 3D data or range data from a single view. We suggest a *volumetric* graph representation of the object, where the nodes represent individual parts and the edges represent connectivity information. We suggest the use of properties of the parabolic curves for performing the part decomposition. We currently consider parts with tubular structure with a straight or curved axis. The graph description presents a structural description of the shape in terms of parts and their arrangement. We are also interested in the internal description of the parts. We study two well defined classes of shapes, namely Straight Homogeneous Generalized Cylinders, and Planar Right Constant GCs. We suggest the use of properties of the parabolic curves for recovering natural descriptions of these classes in terms of their cross sections and axes.

1 Introduction

1.1 Background

We address the recovery of *segmented volumetric* descriptions of 3D shapes. Shape description is the basis for recognition, and is one of the key problems in machine perception. As discussed by many authors (e.g. [4, 16, 17, 12, 22, 24]), the requirements from good shape descriptions lead to descriptions which are segmented, that is given in terms of their parts and parts arrangement. This is also suggested by the study of human perception [3, 19].

The problem of obtaining descriptions of 3D shapes has received considerable attention. Several researchers

have addressed the problem using 2-D image contours as input (e.g. [14, 6, 21, 29, 1, 31]), while others have used range data as input (e.g. [19, 28, 18, 7, 25]). Due to the difficulty of the problem, assumptions are usually made, restricting the type of objects viewed to be either a restricted class of Generalized Cylinders (GCs) or other basic components (e.g. geons [3]), or to possess certain properties such as symmetries.

Several researchers have suggested superquadrics as a tool for shape description [19, 27, 5, 9]. Most of the research in this area has concentrated on finding the best superquadric to fit the given data. The issue of segmentation of the shape into the parts is ignored in most work in this area.

Dickinson *et al.* [7] address the problem of recognizing compound objects which are composed of a limited set of primitives (a subset of Biederman's geons [3]). These primitives can be recovered based on their aspect graph. The assumption in this work, as in most cases where compound objects are handled (e.g. [1, 13]), is that there is a discontinuity edge separating the primitives. This assumption translates into a problem of volumetric descriptions, given that the components are already segmented.

Recent theoretical work has produced several important results regarding the properties of certain GCs and their projections [21, 29, 31]. These properties can be used to recover the 3D information of a simple observed GC. The issues of compound objects which are composed of several of these GCs are not addressed. Compound objects are far more complex than their GC components, since even though the individual components have certain mathematical properties, these properties do not hold for the shape as a whole.

1.2 Issues and approach

We are interested in producing *natural* descriptions of three dimensional *compound* shapes. It is clear that this problem involves two interconnected tasks, namely, the decomposition of the shape into parts, and the description of these parts.

Decomposition As discussed above, most of the work on 3D shapes so far has concentrated on the recovery of descriptions of single components. When compound shapes are addressed, the segmentation is assumed to be an easy step. We attempt to handle compound shapes

*This research was supported by the Advanced Research Projects Agency of the Department of Defense and was monitored by the Air Force Office of Scientific Research under Contract No. F49620-90-C-0078. The United States Government is authorized to reproduce and distribute reprints for governmental purposes notwithstanding any copyright notation hereon.

[†]Currently with the Image Analysis Systems Group, Jet Propulsion Laboratory, MS 168-522, 4800 Oak Grove Drive, Pasadena, CA 91109.

Figure 1: Outline of our approach

2 Segmented Description of Compound Objects

In this section we address the problem of recovering segmented volumetric descriptions of generic compound shapes. As discussed earlier, previous approaches have either addressed special classes of mathematically well defined shapes or they have assumed the segmentation to be given.

When convex parts are combined smoothly, unless there is an accidental alignment, there is an anticlastic (negative Gaussian curvature) annular region between them (the transversality principle). This region gives rise to the matched concavities, which have been used as indication for part segmentation of 2D shapes [12, 3, 1, 24]. In an analogous way to our 2D approach [24], we suggest the use of the parabolic curves for performing the part decomposition. When considering more complex parts, such as tori, tubes or “snake like” shapes, then there could be parabolic curves within the parts and not only on the “glue” between them. Based on the classification of the parabolic curves we can still perform the decomposition.

2.1 From Image to Segmented Surface Description

Given the 3D surface data, we perform the following steps to recover the graph description:

- First, we recover the differential geometric properties of the surface. We recover the derivatives and normals to the surface, the principal directions, and the sign of the Gaussian curvature. It has been shown that this process is stable and reliable [2, 20, 8, 10]. However, in the case of range data input, considerable amounts of smoothing are necessary as an initial step.
- Next, connected regions with the same Gaussian curvature sign are found. A region based graph is then generated, where the nodes are the different

Figure 2: A shaded range image of a teapot (left) and the segmented regions (right).

connected regions and the edges connect neighboring regions and represent the parabolic curves.

The graph recovered at this step is similar to graphs suggested by other researchers (e.g. [8, 18, 11]). This graph is a surface based description and not a volumetric description. It is not at all clear how to make the leap from this surface based description to the desired volumetric description. Consider for example the case of the teapot shown in Figure 2. The original shaded range image is shown on the left, and the segmented regions are shown on the right. The problem of this description is that some regions have no “meaning” by themselves. For example regions 3, 4, and 5 are not independent entities, but belong to the same part, the spout. How does one make this distinction?

2.2 From Surface to Volumetric Description

Basic shapes and parabolic curves Before describing our method for constructing the volumetric description, we introduce some basic generic shape components and the different types of parabolic curves, which we use for constructing the description. These shape components exhaust many, if not most, of the types of shape one is likely to encounter. We follow Koenderink [15] in the selection of these examples and in the terminology used.

Dimple The dimple is a concavity inside an ovoidal shape. For example, if you take a lump of clay and push your thumb in. The concavity is surrounded by an annular hyperbolic (negative Gaussian curvature) region.

Bell The bell is a convex “wart” or part on a globally ovoidal shape. An example is a pare shape. The “bell” is also surrounded by an annular hyperbolic region.

Furrow The Furrow is a hyperbolic region, or dent, in an overall ovoidal shape. Note that this is not a concavity, as the dimple (you cannot hold water in it). An example for this type is a “kidney bean.” This region is surrounded by a single closed parabolic curve.

Hump The hump is a convex region within a larger hyperbolic region. This could be viewed as the opposite of the Furrow which is a hyperbolic region within a convex shape.

These regions are surrounded by parabolic curves, which are the curves of inflection of the Gaussian curva-

ture. There are two cases of such parabolic curves. In the “normal” case, as in the Bell, the lines of curvature which inflect on the parabolic curve (the lines which generate the parabolic curve), are close to being orthogonal to the parabolic curve. We will refer to the parabolic curves of this type as being “part-like.” In the second case, for sections of the parabolic curves, the lines of curvature which inflect on the parabolic curve, are close to being parallel to the parabolic curve. This is the case for the Hump, the Furrow, and also for the outer parabolic curve surrounding the dimple. We will refer to this type of parabolic curve as being “hump-like.” As an illustration, consider an “infinitesimal ant” walking in an orthogonal direction to the parabolic curve on the surface of the Bell. This ant will “feel” an inflection of the curvature when it crosses the parabolic curve. On the other hand, a sister ant walking in the same direction on the Hump, will not feel any inflection when crossing the parabolic curve.

From Surface graph to Volumetric graph In the following steps we construct the part based volumetric graph from the surface graph obtained above.

- First, the parabolic curves are recovered from the borders between the positive and negative regions.
- We now classify the parabolic curves. As discussed above, we distinguish between two cases. In the first case, the lines of curvature, which inflect on the parabolic curve, are close to being orthogonal to the parabolic curve. This case suggests the existence of a part. In the second case, along a section of the parabolic curve, the inflecting lines of curvature, are close to being *parallel* to the parabolic curve. This case suggests that the bordering regions belong to the same part. The actual classification process is implemented as follows: First, the tangent direction to each point of the parabolic curve is computed. The difference between the tangent direction and the direction of the inflecting line of curvature at each point is computed. The point is labelled according to whether this difference is closer to 0 or to 90 degrees. We then filter the labels using a majority filter of width 5 to eliminate random noise effects. Finally, if after the filtering there is a section which is labelled as close to parallel, then the parabolic curve is labelled as “hump-like,” otherwise it is labelled as “part-like.”
- Finally, we generate the part based graph description from the region based graph, obtained earlier, in the following way: We combine regions which share a “hump-like” parabolic curve into a single node. These nodes are hypothesized as being “tube like.” Each negative curvature region connected to two nodes is hypothesized as being “glue.” The positive regions are hypothesized as being convex parts. Negative regions surrounded by a single “hump-like” parabolic curve are labelled as “furrows.”

Figures 3 through 8 follow the whole process on two examples, a teapot, shown on the left side, and a torus shown on the right. Figure 3 shows the shaded range images of the teapot (shown earlier) and torus. This is

Figure 8: Final graph description of teapot (left) and torus (right).

the input to our system. Note that the knob on the lid of the teapot is actually disconnected making it an independent object. Figure 4 shows the images of the sign of the Gaussian curvature of the respective shapes. The borders between the regions are the parabolic curves. Based on the sign of the Gaussian curvature, connected regions are found as shown in Figure 5. The regions graphs obtained at this stage are depicted in Figure 6. Next, the parabolic curves are classified into “hump-like” and “part-like”, as discussed above. The parabolic curves and their classification are shown in Figure 7. Finally, the volumetric part based graphs of the teapot and torus are shown in Figure 8.

3 Axial Description of Parts

In the previous section we have presented a method for recovering a segmented graph description of compound objects. This graph represents the different parts and their arrangement, and it can be used for indexing into a database of objects. For many applications this information may not be sufficient. For example, when trying to grasp an object it is important to have a description of the parts themselves. In this section we discuss the recovery of descriptions of some basic components.

The most simple components are convex blobs. These could be represented in numerous ways (e.g. superquadrics [27]), and we do not address them further. The components we are interested in are tubular structures with a straight or a curved axis. In the following, we discuss two classes of well defined shapes, SHGCs and PRCGCs. Both of these classes could be described naturally by their axis and cross sections. We show how based on known and novel properties of these classes of shapes, we can recover their axes and cross sections.

Unfortunately, not all parts are perfect SHGCs and PRCGCs. It is clear that these techniques could not be used to describe all possible parts. However, in practice, many parts are only slight deformations of the above classes and, therefore, these methods could still result in meaningful descriptions.

3.1 Straight Homogeneous Generalized Cylinders

A *Straight Homogeneous Generalized Cylinder (SHGC)* [26] is a GC with a straight axis and the scaling of the cross section as it is swept along the axis is homogeneous. Figure 9 shows examples of SHGCs. The properties

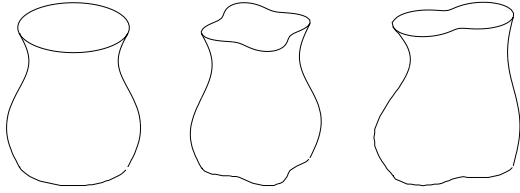


Figure 9: Examples of Straight Homogeneous Generalized Cylinders (adapted from [29]).

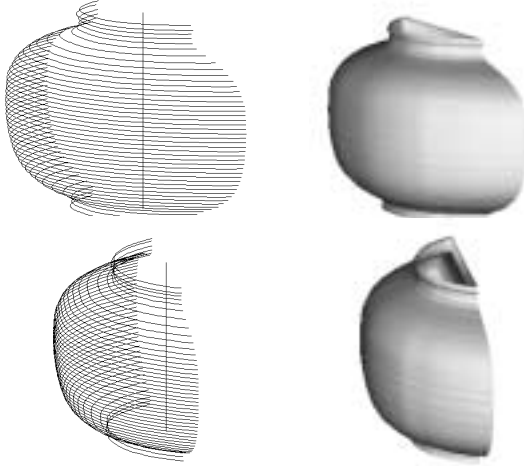


Figure 10: Cross sections and axis (left) and the shaded image (right) of reconstructed teapot body at two different orientations.

of SHGCs have been studied by several researchers (e.g. [26, 21, 29, 31]). We briefly describe here how we recover the axis and cross sections of SHGCs based on some of these properties (refer to [23] for more details).

Given an SHGC, we first recover the parabolic curves on its surface. If it does not have parabolic curves then it is either simply a convex blob, or it has zero Gaussian curvature everywhere. Both cases are not of interest here. Ponce *et al.* [21] have shown that the parabolic curves are either cross sections or meridians of the SHGC. There are a few simple tests which can be done to classify the parabolic curves. From the cross sections found we can recover the axis, by computing the intersection of their correspondence lines [31].

In the case where the cross section sweeping function has no inflections, there are no parabolic curves which are cross sections. However, since the meridians are planar and the axis is in all the meridians planes, the axis can be recovered from the intersection of the meridian planes.

We demonstrate the reconstruction on the real range image of the teapot in Figure 3. The body of the teapot is an SHGC. The parabolic curves, which are also cross sections, were recovered and classified, as discussed in Section 2. A meridian was recovered by traversing the data in an orthogonal direction to a point on one of the cross sections. This meridian conveys the scaling of the sweeping function. We reconstruct a 3-D model of the SHGC by sweeping the cross section along the axis, while scaling it according to the scaling of the sweeping func-

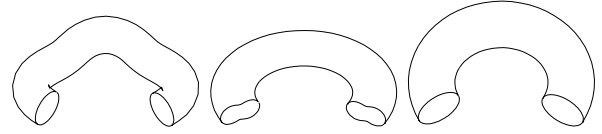


Figure 11: Examples of Planar Right Constant Generalized Cylinders (adapted from [29]).

tion. Figure 10 shows the cross sections and axis and the shaded image of the reconstructed 3-D teapot body. To illustrate the 3-D reconstruction, the results are shown at two novel orientations. Note that since the input is from only one view, we have no information about the “back” of the object. By making assumptions on the symmetrical nature of objects, one could infer a complete (and in this case correct) reconstruction.

3.2 Planar Right Constant Generalized Cylinders

A *Planar Right Constant Generalized Cylinder (PRCGC)* [30] is a GC with a planar axis, a constant cross section, and the cross section is orthogonal to the axis. Figure 11 shows examples of PRCGCs. Although very useful in modeling “tube like” objects, PRCGCs have received relatively little attention [26, 22, 30].

In the following, we first present the formulation for the Gaussian curvature of PRCGCs. This will be used to derive two important properties of PRCGCs. We then show how these properties are used for recovering the axis and cross sections from the 3-D data.

3.2.1 The Gaussian curvature of PRCGCs

Consider a PRCGC. Following the notation used in [30] (refer to Figure 12), we choose a coordinate system, such that the axis of the PRCGC, $A(t) = (a_x(t), 0, a_z(t))$, lies in the $x - z$ plane, and one of the cross sections, $C(u) = (c_x(u), c_y(u), 0)^t$, is in the $x - y$ plane. We also let $A(0) = (0, 0, 0)^t$ and since the cross section is orthogonal to the axis $A'(0) = (0, 0, 1)^t$. The surface of the PRCGC, $S(u, t)$, is then given by:

$$S(u, t) = R(A'(0), A'(t)) \cdot C(u) + A(t) \quad (1)$$

where $R(V_1, V_2)$ is the rotation matrix that transforms the vector V_1 into vector V_2 . For $A'(0) = (0, 0, 1)$ and $A'(t) = (a'_x(t), 0, a'_z(t))$ the rotation matrix R becomes:

$$R = \begin{bmatrix} a'_z(t) & 0 & a'_x(t) \\ 0 & 1 & 0 \\ -a'_x(t) & 0 & a'_z(t) \end{bmatrix}$$

The curves generated by fixing u and varying t are the *meridians* of the surface. The curves generated by fixing t and varying u are the cross sections.

From standard differential geometry, the Gaussian curvature of a surface, K , is given by

$$K = \frac{LN - M^2}{EG - F^2} \quad (2)$$

where E, F, G and L, M, N are the coefficients of the first and second fundamental forms respectively. In the

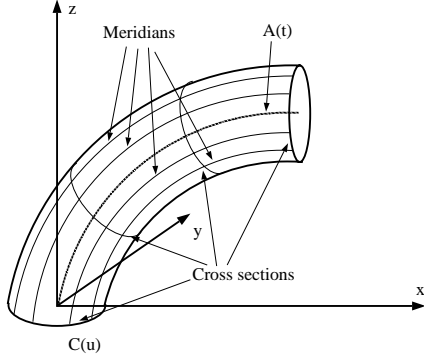


Figure 12: A PRCGC with some meridians and cross sections marked (adapted from [29]).

case of the PRCGC they are given by the following equations (refer to [23] for the complete computational details):

$$\begin{aligned}
 E &= S_u \cdot S_u = 1 \\
 F &= S_u \cdot S_t = 0 \\
 G &= S_t \cdot S_t = (1 - K_A c_x)^2 \\
 L &= S_{uu} \cdot n = -K_C \\
 M &= S_{ut} \cdot n = 0 \\
 N &= S_{tt} \cdot n = -(1 - K_A c_x) K_A c'_y
 \end{aligned} \quad (3)$$

where $K_A = K_A(t)$ and $K_C = K_C(u)$ denote the curvature of the axis and cross section respectively.

From equations 2 and 3 the Gaussian curvature of a PRCGC is given by

$$K = K(u, t) = -\frac{1}{\gamma(u, t)} K_A(t) K_C(u) c'_y(u) \quad (4)$$

where $\gamma(u, t) = 1 - K_A c_x$. Note that since we assume that the PRCGC does not intersect itself, γ is strictly positive.

3.2.2 Properties of PRCGCs

We can now prove a property, which relates the parabolic curves of a PRCGC to its axis, meridians, and cross section. This is a property is very useful in recovering the axis and cross sections of a PRCGC.

Property 3.1 *Parabolic curves on the surface of a PRCGC are the cross sections where the curvature of the axis is zero, and they are meridians where either the curvature of the cross section is zero, or when the tangent to the cross section is parallel to the axis plane.*

Proof From Equation 4 it is clear that the Gaussian curvature of the surface, $K(u, t)$, of a PRCGC is zero if and only if

1. the curvature of the axis, $K_A(t)$, is zero for some t_0 , in which case the corresponding cross section, $S(u, t_0)$, is a parabolic curve, or,
2. the curvature of the cross section, $K_C(u)$, is zero for some u_0 , in which case the corresponding meridian $S(u_0, t)$ is a parabolic curve, or,
3. the tangent to the cross section is parallel to the axis plane, $c'_y(u_0) = 0$ for some u_0 , in which case the corresponding meridian $S(u_0, t)$ is a parabolic curve. \square

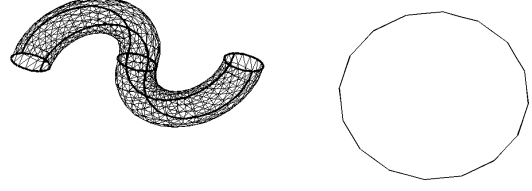


Figure 13: A PRCGC (left) and the recovered cross section (right). The parabolic curves (and the terminations) are shown emphasized.

Based on the coefficients of the first and second fundamental forms in Equation 3 we can derive the following important property of PRCGCs. This property is well known for the specific case of the torus, but, to the best of our knowledge, was never stated for more general PRCGCs.

Property 3.2 *The meridians and cross sections of a PRCGC are its lines of curvature.*

Proof From standard differential geometry we know that the parameter curves in the neighborhood of a non-umbilical point are lines of curvature if and only if $F = M = 0$. Based on Equation 3 this condition holds for the above u and t parameterization of the PRCGC where, as noted, the u parameter curves are the cross sections and the t parameter curves are the meridians. \square

3.2.3 Recovering the axis and cross section of a PRCGC

The above properties suggest two methods for recovering the cross section and the meridians of a PRCGC. One possibility, based on Property 3.2, is to compute the lines of curvature on the surface, which are the cross sections and meridians. To recover the cross section, it is actually sufficient to compute the principal directions at any point on the surface and cut the object along them. The other possibility, based on Property 3.1, is to recover the parabolic curves which are also either meridians or cross sections. We have used the second method in our experiments. Note that a PRCGC must always have at least two parabolic curves (unless it is the degenerate case of a straight axis and convex cross section). As in the case of the SHGC, there are a few simple tests which can be done to classify the parabolic curves and the lines of curvature.

The cross section and meridians of a PRCGC give a complete description of it, since any curve parallel to the meridians could be the axis. We define the most intuitive axis to be the one passing through the center of the cross section (or center of gravity for a non-circular cross section).

Figures 13 and 14 show results on two complete, synthetic PRCGCs. In both images the PRCGC is shown on the left. The parabolic curves and the terminations are emphasized with thicker lines. In the case of the PRCGC of Figure 14 only the top five parabolic curves are emphasized to avoid cluttering of the image. In both instances, the recovered cross-sections are shown on the right.



Figure 14: A PRCGC (left) and the recovered cross section (right). The top parabolic curves (and the terminations) are shown emphasized.

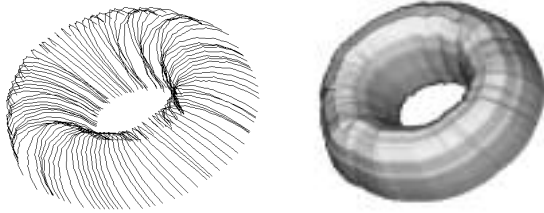


Figure 15: Cross sections and shaded image of reconstructed torus.

Finally, we turn back to our examples of real range images of the teapot and torus (Figure 3). The torus and the handle of the teapot are nearly perfect PRCGCs. The parabolic curves were recovered and classified, as discussed in Section 2 (see Figure 7). A cross section is recovered by traversing the data in an orthogonal direction from a point on the meridian. Finally, we reconstruct a 3-D model of the PRCGC by sweeping the cross section along the meridian. To illustrate the reconstruction we show the results at different orientations. Figure 15 shows the cross sections and shaded image of the reconstructed 3-D torus, while Figure 16 shows the cross sections and shaded images of the reconstructed teapot handle at two different orientations.

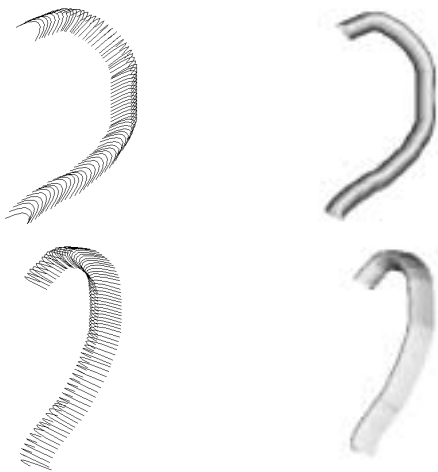


Figure 16: Cross sections and shaded image of reconstructed teapot handle at two different orientations.

4 Concluding remarks

We have addressed the problem of obtaining natural volumetric descriptions of three dimensional shapes. We address compound shapes where the components are connected smoothly. We use the parabolic curves for segmenting the shape into its components. We currently handle parts with tubular structure. We generate a graph where the nodes represent the individual parts. This graph presents a structural description of the shape in terms of parts and their arrangement. We have also presented methods for recovering the axis, meridians and cross sections of SHGC and PRCGC components, based on known and novel mathematical properties.

We have presented some preliminary, but promising results. Some more tests are still necessary and are currently underway. The issues of recovering the description from a single range image are also not completely addressed. Extensions to other classes of components are also under investigation.

Acknowledgment

We would like to thank Mourad Zerroug for his help with proving the properties of the PRCGCs.

References

- [1] R. Bergevin and M. D. Levine. Part decomposition of objects from single view line drawings. *Computer Vision, Graphics and Image Processing*, 55:73–83, January 1992.
- [2] P. J. Besl and R. C. Jain. Invariant surface characteristics for 3D object recognition in range image. *Computer Vision, Graphics and Image Processing*, 33:33–80, 1986.
- [3] I. Biederman. Recognition by components. *Psychological Review*, 94:115–147, 1987.
- [4] T. O. Binford. Visual perception by computer. In *IEEE Conference on Systems and Controls*, Miami, FL, 1971.
- [5] T. E. Boult and A. D. Gross. On the recovery of superellipsoids. In *Proceedings of the DARPA Image Understanding Workshop*, pages 1052–1063, Cambridge, MA, 1988.
- [6] R. A. Brooks. Symbolic reasoning among 3-D models and 2-D images. *Artificial Intelligence*, 17:285–348, 1981.
- [7] S. J. Dickinson, A. P. Pentland, and A. Rosenfeld. 3-D shape recovery using distributed aspect matching. *IEEE Transactions on Pattern Analysis and Machine Intelligence*, 14(2):173–199, February 1992.
- [8] T. J. Fan, G. Medioni, and R. Nevatia. Recognizing 3-D objects using surface descriptions. *IEEE Transactions on Pattern Analysis and Machine Intelligence*, 11(11):1140–1157, 1989.
- [9] F. P. Ferrie, J. Lagarde, and P. Whaite. Recovery of volumetric object descriptions from laser rangefinder images. In *Proceedings of European*

- Conference on Computer Vision*, pages 387–396, Antibes, France, 1990.
- [10] P. J. Flynn and A. K. Jain. On reliable curvature estimation. In *Proceedings of IEEE Conference on Computer Vision and Pattern Recognition*, pages 110–116, San Diego, CA, June 1989.
- [11] P. J. Flynn and A. K. Jain. 3D object recognition using invariant feature indexing of interpretation tables. In *IEEE Workshop on Directions in Automated CAD-Based Vision*, pages 115–123, Maui, Hawaii, June 1991.
- [12] D. D. Hoffman and W. A. Richards. Parts of recognition. *Cognition*, 18:65–96, 1985.
- [13] J. E. Hummel and I. Biederman. Dynamic binding in a neural network for shape recognition. *Psychological Review*, 99:480–517, 1992.
- [14] J. J. Koenderink. What does the occluding contour tell us about solid shape. *Perception*, 13:321–330, 1984.
- [15] J. J. Koenderink. *Solid Shape*. MIT Press, 1990.
- [16] D. Marr. *Vision*. W. H. Freeman and Co., San Francisco, CA, 1982.
- [17] R. Nevatia. *Machine Perception*. Prentice Hall, 1982.
- [18] B. Parvin and G. Medioni. A dynamic system for object description and correspondence. In *Proceedings of IEEE Conference on Computer Vision and Pattern Recognition*, pages 393–399, Maui, Hawaii, June 1991.
- [19] A. P. Pentland. Recognition by parts. In *Proceedings of IEEE International Conference on Computer Vision*, pages 612–620, London, England, June 1987.
- [20] J. Ponce and M. Brady. Towards a surface primal sketch. In T. Kanade, editor, *Three Dimensional Machine Vision*, pages 195–239. Kluwer Academic, New York, 1987.
- [21] J. Ponce, D. Chelberg, and W. B. Mann. Invariant Properties of Straight Homogeneous Generalized Cylinders and Their Contours. *IEEE Transactions on Pattern Analysis and Machine Intelligence*, 11(9):951–966, 1989.
- [22] K. Rao. *Shape Description from Sparse and Imperfect Data*. PhD thesis, University of Southern California, December 1988. IRIS Technical Report 250.
- [23] H. Rom. *Part Decomposition and Shape Description*. PhD thesis, University of Southern California, December 1993. IRIS Technical Report 93-319.
- [24] H. Rom and G. Medioni. Hierarchical decomposition and axial shape description. *IEEE Transactions on Pattern Analysis and Machine Intelligence*, 15(10):973–981, 1993.
- [25] Y. Sato, J. Ohya, and K. Ishii. Smoothed local generalized cones: An axial representation of 3D shapes. In *Proceedings of IEEE Conference on Computer Vision and Pattern Recognition*, pages 56–62, Champaign, Illinois, June 1992.
- [26] S. A. Shafer. Shadow geometry and occluding contours of generalized cylinders. Technical Report CMU-CS-83-131, Carnegie-Mellon University, May 1983.
- [27] F. Solina. *Shape Recovery and Segmentation with Deformable Part Models*. PhD thesis, University of Pennsylvania, 1987.
- [28] D. Terzopoulos, A. Witkin, and M. Kass. Symmetry-seeking models for 3D object reconstruction. In *Proceedings of IEEE International Conference on Computer Vision*, pages 269–276, London, England, June 1987.
- [29] F. Ulupinar and R. Nevatia. Shape from contour: SHGCs. In *Proceedings of IEEE International Conference on Computer Vision*, pages 582–582, Osaka, Japan, 1990.
- [30] F. Ulupinar and R. Nevatia. Recovering shape from contour for constant cross section generalized cylinders. In *Proceedings of IEEE Conference on Computer Vision and Pattern Recognition*, pages 674–676, Maui, Hawaii, 1991.
- [31] M. Zerroug and R. Nevatia. Volumetric descriptions from a single intensity image. *International Journal of Computer Vision*, 1993. (To appear).